Comp Clin Pathol (2008) 17:51–54
DOI 10.1007/s00580-007-0705-z

ORIGINAL ARTICLE

Intraerythrocytic inclusion bodies in painted turtles (*Chrysemys picta picta*) with measurements of affected cells

Andrew K. Davis · Kerry L. Holcomb

Received: 13 August 2007 / Accepted: 19 September 2007 / Published online: 20 October 2007

Abstract We report the discovery and description of intraerythrocytic inclusion bodies of unknown classification in blood films of six painted turtles (*Chrysemys picta picta*) from a pond in northeast Georgia. All six individuals examined were of adult size and appeared to have no outward signs of disease or abnormalities, but all had inclusions with the prevalence of erythrocytes affected within individuals ranging from 6.1 to 34.2% of erythrocytes. Under light microscopy, the inclusion bodies appeared light blue with Giemsa staining, were approximately round in shape, and were only observed singly in erythrocytes. Inclusions were typically located near the nucleus, but the nucleus of affected cells was not abnormally positioned because of the inclusion. No vacuoles, granules, or crystalline structures were observed in association with the inclusions. Measurements via image analysis determined that inclusion bodies ranged from 0.6 to 1.3 μm in diameter. Measurements of erythrocyte dimensions indicated that affected erythrocytes were significantly longer, narrower, and smaller in area than unaffected cells, suggesting that the inclusions were associated with mature cells. Further, larger inclusion bodies tended to be associated with narrower cells, which may indicate that inclusions become larger as cells age.

Keywords Intraerythrocytic · Inclusion bodies · Painted turtle · *Chrysemys picta picta* · Reptile erythrocytes

A. K. Davis (✉) · K. L. Holcomb
Warnell School of Forestry and Natural Resources,
University of Georgia,
Athens, GA 30602, USA
e-mail: akdavis@uga.edu

Introduction

Intraerythrocytic inclusion bodies have been noted in the blood of several species of reptiles, especially in snakes (Daly et al. 1980; Smith et al. 1994; Johnsrude et al. 1997), although the nature of their classification has been debated. There are various organisms that can manifest as small, often rounded, structures within erythrocytes, most notably viruses (e.g., Telford and Jacobson 1993). For example, iridoviral infections are characterized by numerous hexagonal-shaped inclusions (Johnsrude et al. 1997). Moreover, organisms in the genus *Toddia* also form inclusion bodies and were once thought to be protozoa but are now known as 'snake erythrocytic viruses' (Smith et al. 1994). In addition, Smith et al. (1994) found that these inclusions tended to be in more rounded cells. Similarly, *Pirhemocyton* sp. appear as small round inclusions and were once thought to be piroplasms but are now known as 'lizard erythrocytic viruses' (Telford and Jacobson 1993). In both of these cases, the infections are typified by small, round, red-staining inclusions in Giemsa-stained erythrocytes (Telford and Jacobson 1993; Smith et al. 1994) and are associated with vacuole and basophilic-staining particles (Daly et al. 1980). Species of *Pirhemocyton* have also been noted in turtles, with observations of light pink staining, a central chromatid dot in the inclusion, and a ring of granules around or trailing behind the inclusion (Acholonu 1974). Finally, Eiras et al. (2000) reported intraerythrocytic inclusions of unknown etiology in loggerhead sea turtles that were not consistent with *Toddia* or *Pirhemocyton* sp. The reported inclusions in that case stained uniformly deep blue and were not associated with vacuoles or crystals (Eiras et al. 2000).

While preparing blood films of a set of six wild-caught painted turtles (*Chrysemys picta picta*) from northeast

Georgia for an unrelated study, we noticed intraerythrocytic inclusions consistent with that described by Eiras et al. (2000). We subsequently conducted the following light microscopy study, where we describe the characteristics of the inclusions, their prevalence in erythrocytes within individuals, and using image analysis, their size, and the morphology of affected cells and unaffected cells, which we compared statistically. We further examined if the size of inclusions varied with the dimensions of erythrocytes.

Materials and methods

Capturing and sampling turtles

Turtles were captured using hoop traps that were set along the bank of a permanent pond in the University of Georgia's Whitehall Experimental Forest near Athens GA (33°57′N, 83°19′W). A total of six turtles were captured, three males and three females, all in the month of July of 2007. When captured, the carapace length of each was measured, and all were within the size range of adults for *Chrysemys* sp. (Rowe et al. 2003). Within 10 min of capture of each turtle, we obtained a blood sample with a clean 23-gauge syringe from the subcarapacial junction of the common intercostals vein and the caudal cervical branch of the external jugular vein, a venipuncture site described by Hernandez-Divers et al. (2002). A blood smear was then made using two clean microscope slides by drawing a drop of blood across one slide with the other. Slides were then air-dried and later stained with Giemsa. Turtles were released after blood sampling at the site of capture.

Screening blood smears

In the laboratory, we initially examined all blood smears under low magnification to identify common blood parasites such as Hemoprotozoa (Strohlein and Christensen 1984; Jakes et al. 2001), although we did not identify these parasites to species. Thereafter, we examined each smear under 1,000× (oil) and randomly selected ten clear fields of view. We counted all erythrocytes visible in the field and recorded the number of cells containing inclusion bodies.

Measuring erythrocytes and inclusions

We measured a subset of erythrocytes with and without inclusions using an image analysis approach similar to that used previously to measure erythrocyte dimensions of salamanders (Davis 2007). We examined one blood smear under 1,000× (oil) and randomly selected 20 fields of view, which we photographed using a Canon Powershot G6 digital camera mounted on the microscope. The blood images were imported into Fovea Pro (Reindeer Graphics), an image analysis software package, and all visible cells with and without inclusions were selected and their dimensions (length, width, area, and aspect ratio) measured. Furthermore, we also measured the nucleus dimensions of affected and unaffected cells. Finally, we measured the diameter (i.e., length of longest axis) and two-dimensional area of the inclusion bodies themselves in affected erythrocytes.

Data analysis

To determine if the inclusion bodies were associated with certain erythrocyte dimensions, we compared the cell length, width, area, and aspect ratio of affected and unaffected cells using two-sample *t* tests. We similarly compared the same nuclear dimensions of affected and unaffected cells. To determine if inclusion body size varied with any aspect of erythrocyte morphology, we used Pearson correlation to compare each erythrocyte dimension against inclusion body area. Tests were performed using Statistica 6.1 software (Statistica 2003).

Results

General observations

The inclusion bodies appeared light to dark blue under 1,000× magnification and generally had a round shape.

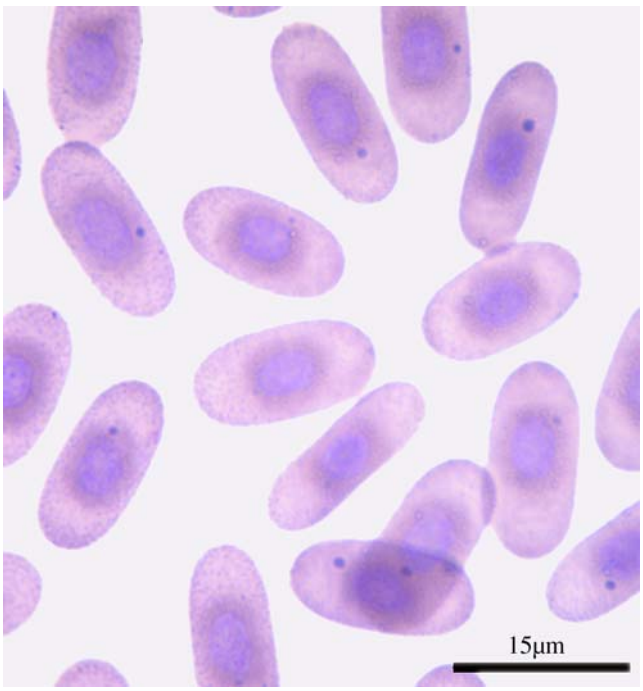

Fig. 1 Photomicrograph of painted turtle erythrocytes with and without inclusion bodies, under 1,000× magnification

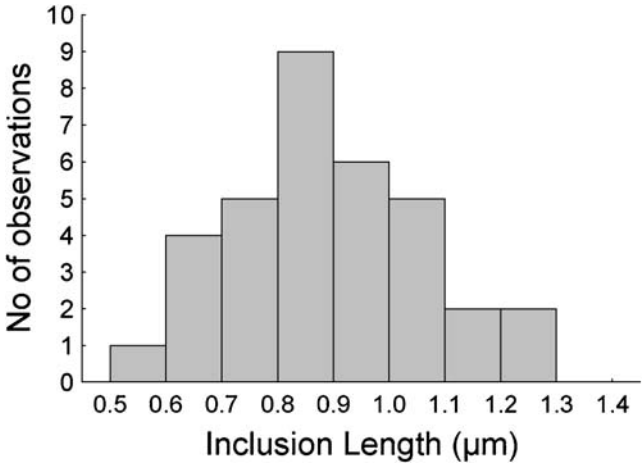

Fig. 2 Frequency-distribution of inclusion body length (i.e., diameter). A total of 34 inclusion bodies were measured

Furthermore, they only appeared singly in affected erythrocytes (Fig. 1). The nucleus of affected cells appeared to be centrally positioned in all cases (i.e., the inclusion did not push the nucleus to the side). The inclusion bodies themselves were usually positioned near the nucleus but occasionally were located midway between the nucleus and the cell membrane. They were rarely located next to the membrane. The inclusion bodies varied in size, ranging from 0.6 to 1.3 μm in diameter, with a mean of 0.89 μm (Fig. 2). We observed no vacuoles or crystalline structures associated with the inclusions. Finally, we noted that four of the turtles also had infections of *Hemoproteus* sp., and in one turtle, we observed *Leucocytozoan* sp., although there was no apparent relationship between blood parasite presence and inclusion body presence, especially given that all six turtles had inclusion bodies.

Prevalence of inclusions

The number and prevalence of inclusion bodies in all six turtles is shown in Table 1. While the number of cells examined varied due to variation in smear density, the prevalence of inclusions ranged from 6.1 to 34.5%, with a mean of 17.5%. While too few turtles were examined to allow for statistical comparisons male vs female prevalence, we did note that the two highest prevalence values were both in female turtles. Further, there did not appear to be an association between prevalence and turtle body size (carapace length).

Table 1 Summary of painted turtles examined in this study, with prevalence of inclusion bodies in erythrocytes of each turtle

Turtle number	Sex	Carapace length (mm)	No. of cells examined	No. with inclusions	Prevalence (%)
1	Female	140	427	146	34.2
2	Female	142	1,121	85	7.6
3	Female	137	330	112	33.9
4	Male	135	719	111	15.4
5	Male	132	327	20	6.1
6	Male	150	450	36	8.0
Average			562	85	17.5

A total of ten randomly selected fields of view (under 1,000×) were examined for each individual.

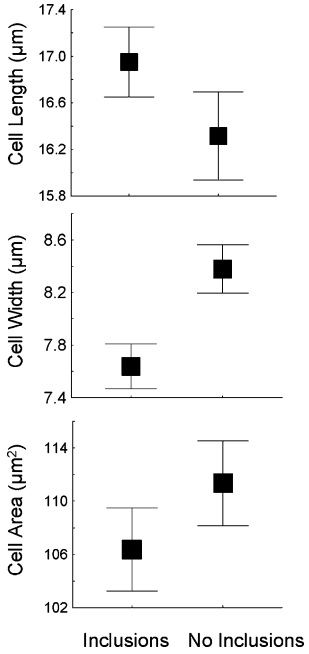

Fig. 3 Dimensions of erythrocytes with and without inclusion bodies, including cell length (*top*), width (*middle*) and two-dimensional surface area (*bottom*), measured with image analysis routines. Shown are the means plus 95% confidence intervals for each group

Erythrocyte measurements

Erythrocytes without inclusion bodies (n=42) ranged in length from 13.8 to 19.2 μm with a mean of 16.3 μm, while those with inclusions (n=34) ranged from 14.8 to 19.0 μm

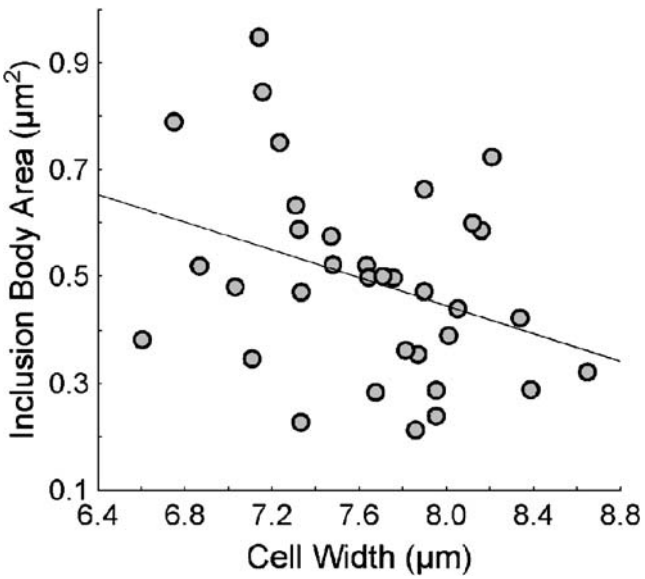

Fig. 4 Scatterplot showing significant negative correlation (r=−0.35, p=0.043) between inclusion body size (area) and erythrocyte width

with a mean of 17.0 μm. This difference was significant (two-sample t test, df=74, t=2.58, p=0.012; Fig. 3, top). Furthermore, erythrocytes with inclusions were significantly narrower than those without (8.4 vs 7.6 μm, df=74, t=−5.86, p<0.001; Fig. 3, middle). Finally, erythrocytes with inclusion bodies were also significantly smaller in terms of (two-dimensional) area (111.3 vs 106.3 μm, df=74, t=−2.23, p=0.029; Fig. 3, bottom). From these results, we conclude that erythrocytes with inclusion bodies tend to be longer, narrower, and smaller than those without. In contrast, nuclei did not vary in length (d=74, t=−0.39, p=0.69), width (df=74, t=−0.08, p=0.940), or area (df=74, t=−0.74, p=0.458). Thus, there were no differences in nuclear dimensions of affected and unaffected erythrocytes.

Inclusion measurements

Using the data from affected cells only, we found no relationship between cell length and inclusion body area (Pearson correlation, r=0.02, p=0.890). There was also no relationship between cell area and inclusion area (r=−0.26, p=0.131). However, there was a significant negative relationship between cell width and inclusion area (r=−0.35, p=0.043; Fig. 4). There were no relationships between inclusion area and nucleus area (r=−0.13, p=0.470), length (r=0.03, p=0.858), or width (r=−0.08, p=0.636).

Discussion

There are several lines of evidence in our study that suggest that the inclusions described in this study are unlike the lizard erythrocytic virus inclusions described by Telford and Jacobson (1993) or the snake erythrocytic virus described by Smith et al. (1994). Importantly, the viral inclusions in both previous cases stained red or pink, while in our case, they were blue under Giemsa stain. Furthermore, Smith et al. (1994) reported that infected erythrocytes tended to be rounder than uninfected; the opposite trend was found in this study. Finally, we observed no vacuoles associated with our inclusions, as was reported by both Smith et al. (1994) and Telford and Jacobson (1993). Interestingly, our inclusions do appear somewhat consistent with that described by Eiras et al. (2000) in loggerhead sea turtles, who described 0.5–2.0 μm, blue-staining, single intraerythrocytic inclusions that caused no apparent deformity in nuclear position. These authors also concluded that their inclusions were not consistent with viral particles but did not know the etiology of the phenomena. We point out however, that while they observed small granular areas in the cytoplasm associated with the inclusions, we did not in this study.

Our comparisons of affected and unaffected cell morphology revealed that affected cells tend to be longer, narrower, and smaller in overall area than unaffected cells, which are all characteristics of more mature cells in non-mammalian erythrocytes (Hawkey and Dennett 1989) This result also speaks to the inconsistency with snake erythrocytic virus, which is reported to be associated with rounder cells (Smith et al. 1994). Regarding cell age, the relationship we found between inclusion body size and erythrocyte width is suggestive of a tendency for inclusions to be larger in older cells. However, the lack of a relationship with other dimensional variables makes this assertion premature at this time. We can conclude that our morphological measurements of erythrocytes and inclusions provide a new perspective on the nature of this phenomenon, which suggests that future studies using this approach should prove fruitful.

Acknowledgements We thank Sean Sterrett and Andrew Grosse for help in catching turtles. AKD was supported by funds from the D.B. Warnell School of Forestry and Natural Resources during this study. Logistic support and equipment were provided by John Maerz.

References

Acholonu AD (1974) Haemogregarina pseudemydis n. sp. (Apicomplexa: Haemogregarinidae) and *Pirhemocyton chelonarum* n. sp. in turtles from Louisiana. J Protozool 21:659–664

Daly JJ, Mayhue M, Menna JH, Calhoun CH (1980) Viruslike particles associated with Pirhemocyton inclusion bodies in the erythrocytes of a water snake, *Nerodia erythrogaster flavigaster*. J Parasitol 66:82–87

Davis AK (2007) Ontogenetic changes in erythrocyte morphology in larval mole salamanders, Ambystoma talpoideum, measured with image analysis. Comp Clin Pathol (in press) DOI 10.1007/s00580-007-0702-2

Eiras JC, Dellinger T, Davies AJ, Costa G, de Matos APA (2000) Intraerythrocytic inclusion bodies in the loggerhead sea turtle *Caretta caretta* from Madeira. J Mar Biol Assoc (UK) 80:957–958

Hawkey CM, Dennett TB (1989) Color atlas of comparative veterinary hematology. Iowa State University Press, Ames, Iowa

Hernandez-Divers SM, Hernandez-Divers SJ, Wyneken J (2002) Angiographic, anatomic, and clinical technique descriptions of a subcarapacial venipuncture site for chelonians. J Herpetol Med Surg 12:32–37

Jakes KA, O'Donoghue P, Munro M, Adlard R (2001) Hemoprotozoa of freshwater turtles in Queensland. J Wildl Dis 37:12–19

Johnsrude JD, Raskin RE, Hoge AYA, Erdos GW (1997) Intraerythrocytic inclusions associated with iridoviral infection in a fer de lance (*Bothrops moojeni*) snake. Vet Pathol 34:235–238

Rowe JW, Coval KA, Campbell KC (2003) Reproductive characteristics of female midland painted turtles (*Chrysemys picta marginata*) from a population on Beaver Island, Michigan. Copeia 2003:326–336

Smith TG, Desser SS, Hong H (1994) Morphology, ultrastructure and taxonomic status of Toddia sp in northern water snakes (*Nerodia sipedon sipedon*) from Ontario, Canada. J Wildl Dis 30:169–175

Statistica (2003) Statistica version 6.1, Statsoft Inc, Tulsa, OK, USA

Strohlein DA, Christensen BM (1984) *Haemogregarina* sp (Apicomplexa, Sporozoea) in aquatic turtles from Murphys Pond, Kentucky. Trans Am Microsc Soc 103:98–101

Telford SR, Jacobson ER (1993) Lizard erythrocytic virus in East African chameleons. J Wildl Dis 29:57–63